Available online at www.sciencedirect.com
SCIENCE DIRECT®
European Journal of Medicinal Chemistry 41 (2006) 457–466
EUROPEAN JOURNAL OF MEDICINAL CHEMISTRY
http://france.elsevier.com/direct/ejmech

Original article

New potent 5-nitrofuryl derivatives as inhibitors of *Trypanosoma cruzi* growth. 3D-QSAR (CoMFA) studies

Gabriela Aguirre [a], Mariana Boiani [a], Eliana Cabrera [a], Hugo Cerecetto [a,*], Rossanna Di Maio [a], Mercedes González [a,*], Ana Denicola [b], Carlos Mauricio R. Sant'Anna [c], Eliezer J. Barreiro [d]

[a] *Departamento de Química Orgánica, Facultad de Química-Facultad de Ciencias, Universidad de la República, Iguá 4225, 11400 Montevideo, Uruguay*
[b] *Laboratorio de Fisicoquímica Biológica, Facultad de Ciencias, Universidad de la República, Iguá 4225, 11400 Montevideo, Uruguay*
[c] *Departamento de Química, ICE, Universidade Federal Rural do Rio de Janeiro, Seropédica, Brazil*
[d] *LASSBIO, Faculty of Pharmacy, University Federal of Rio de Janeiro, Rio de Janeiro, Brazil*

Received 31 May 2005; received in revised form 16 November 2005; accepted 30 November 2005
Available online 23 February 2006

Abstract

Growth inhibitory activity in vitro of sixteen new 5-nitrofuryl derivatives against the protozoan parasite *Trypanosoma cruzi*, the causative agent of American trypanosomiasis, was studied. The designed compounds combine in the same molecule the recognized 5-nitrofuryl group, an oxidative stress promoter, and lateral chains that could interact with biomolecules such as trypanothione reductase. Some of the derivatives were found to be very active against the epimastigote form of the parasite, being near to 3.0-fold more active than the reference compound, nifurtimox. Moreover, three-dimensional requirements for activity were clearly observed using a 3D-QSAR study based on a comparative molecular field analysis (CoMFA). The best CoMFA model, $r^2 = 0.970$ and $q^2 = 0.725$, points to the importance of a specific hydrogen-bonding pattern around the carbonyl or thiocarbonyl moieties, as well as the requirement for hydrophobic lateral chains. Theoretical pharmacokinetics (Lipinski's rule, PSA) supports further in vivo studies.

Keywords: 5-nitrofuryl derivatives; Anti-*T. cruzi* compounds; CoMFA

1. Introduction

Chagas' disease or American trypanosomiasis is an important health problem that affects around twenty million people in Central and South America. Around 2–3 million individuals develop the typical symptoms of this disease that results in 50 000 yearly deaths [1,2]. The causative agent of this disease is the haemoflagellate protozoan *Trypanosoma cruzi* (*T. cruzi*), which is transmitted in rural areas to humans and other mammals by reduviid bugs such as *Rhodnius prolixus* and *Triatoma infestans* [3]. The main route of transmission is the result of blood-sucking activity of Chagas' disease vectors on mammals when feeding in a cyclic process. The parasite presents different morphological forms in a complex life cycle: amastigote, the mammalian multiplicative intra-cellular form; trypomastigote, the non-dividing bloodstream form that invades tissues; metacyclic trypomastigotes, the non-dividing highly infective form that invade mammalian tissues via wounds provoked by vector blood sucking action; epimastigotes, the replicative form that exists in the Chagas' disease vector. Recently, the existence of the epimastigote form as an obligate mammalian intracellular stage has been revisited [4,5] and confirmed [6]. Despite the progress achieved in the study of *T. cruzi* biochemistry and physiology, in which several crucial enzymes for parasite survival, absent in the host, have been identified as potential targets for the design of new drugs [7,8], the che-

* Corresponding author. Tel.: +598 2 525 8618 (ext. 216); fax: +598 2 525 0749.
E-mail addresses: hcerecet@fq.edu.uy (H. Cerecetto), megonzal@fq.edu.uy (M. González).

0223-5234/$ - see front matter © 2006 Elsevier SAS. All rights reserved.
doi:10.1016/j.ejmech.2005.11.008

motherapy to control this parasitic infection remains undeveloped. The pharmacology is based on old and quite unspecific drugs associated with long term treatments that rise to severe side effects. In fact, although nifurtimox (4-([5-nitrofurfurylidene]-amino)-3-methylthio morpholine-1,1-dioxide, Nfx, Scheme 1) and benznidazole (*N*-benzyl-2-nitro-1-imidazoleacetamide, Bnz), the only two drugs currently in use for clinical treatment of this disease, are able to wipe out parasitemia and to reduce serological titters, they are not specific enough to all *T. cruzi* strains and they do not guarantee complete cure. Both drugs act via the reduction of the nitro group. In the case of Nfx, reduction generates an unstable nitro anion radical which produces highly toxic reduced oxygen species whereas Bnz involves covalent modification of macromolecules by nitro reduction intermediates [9]. The side effects of these drugs result from the oxidative or reductive damage in the host's tissues and are thus inextricably linked to its anti-parasitic activity. Despite these limitations, some studies involving nitroimidazole derivatives have been recently described [10,11].

Recently, we have shown that new 5-nitrofuryl derivatives (Table 1) possess a high anti-*T. cruzi* activity in vitro and in vivo [12–15] and we have demonstrated that this family of compounds produces oxidative stress into the parasite as the main mechanism of action [16–19]. Compound **1** and analogues are good examples of the previously reported 3-D QSAR models using in vitro and in vivo anti-*T. cruzi* activities [20]. There, the three dimensional in vitro model was found to be in agreement with the active site of trypanothione reductase from *T. cruzi* [14,21], an NADPH-dependent flavoenzyme involved in trypanosome protection against free radicals [22].

From these biological results some lead compounds for further modifications were selected. Derivatives of 5-nitrofurylacroleine were more active than the corresponding 5-nitrofuryl analogues (compare activities of compounds **2** and **3**, **13** and **17**, and **14** and **18**, Table 1), thus new derivatives were synthesized that contain this ethenyl substituent on the 5-nitrofuryl system (Scheme 1). Since thiosemicarbazone derivatives **12–19**, carbazate derivatives **5–8** and apolar-substituted amides **20** and **21** displayed excellent activities new analogues were also synthesized (Scheme 1).

In the present work, the development of new 5-nitrofuryl derivatives (**26–42**, Schemes 2–4) and their anti-*T. cruzi* activities are described. Theoretical approaches, using CoMFA methodologies, were developed in order to know three-dimensional requirements for optimum activity.

2. Chemistry

The new 5-nitrofuryl containing semicarbazones, **26–29**, and 5-nitrofuryl containing carbazates, **30–34** (Scheme 2) were prepared using the methodology indicated in Scheme 2. A typical procedure consisted in the reaction between 3-(5-nitrofuryl)acroleine (1 equiv.) and the semicarbazide derivative or carbazate derivative (1 equiv.) [23,24], in the presence of catalytic amounts of *p*-toluenesulphonic acid (*p*-TsOH) and dried toluene as solvent, at room temperature.

Amides **35–37** were prepared by following a two-step procedure from the corresponding acid **9**, which was transformed into the intermediate **25** (Scheme 3) [14,25–27]. Treatment of intermediate **25** with different amines at room temperature leads to obtain the desired products in moderate yields.

To prepare thioamides **38–40** the corresponding amides (**20–22**) were irradiated in a conventional microwave oven in the presence of Lawesson's reagent, in a free-solvent process. These derivatives were obtained in a very clean process but in low yields (Scheme 3) [28,29]. No attempt was made to improve these yields.

Furthermore, 5-nitrofuryl and 5-nitrothienyl derivatives, **41** and **42**, previously obtained by us [30,31] were included in the biological studies. These compounds were prepared as is depicted in Scheme 4.

All new compounds were characterised by NMR (^{1}H, ^{13}C, COSY and HETCOR experiments), IR and MS. The purity was established by TLC and microanalysis. Only one stereoisomer was evidenced in solution (NMR studies). The *E*-stereochemistry around carbon–carbon and carbon–nitrogen double bonds was established using the corresponding ^{1}H-NMR coupling constant (*J* around 16.0 and 9.5 Hz [32,33], respectively).

3. Pharmacology

All 5-nitrofuryl derivatives were tested in vitro against *T. cruzi*, Tulahuen 2 strain, as previously described [34]. The compounds were incorporated into the media at 5 μM and their

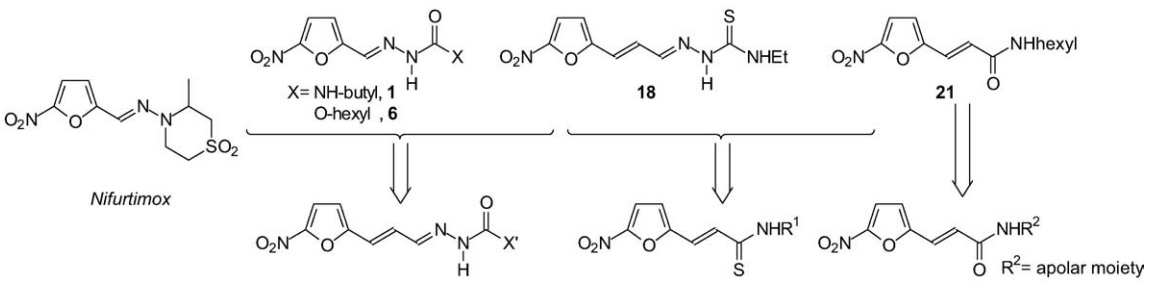

Scheme 1. Design of new 5-nitrofuryl analogues.

Table 1
Family of developed 5-nitrofuryl derivatives and in vitro anti-*T. cruzi* behaviour

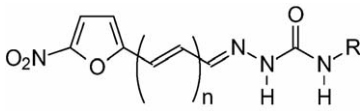

Compound	*n*	–R	$\log_{10}$ PGI [a]
1	0	$–CH_2CH_2CH_2C–H_3$	1.32
2	H_3	–H	1.78
3	1	–H	1.81

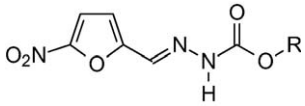

Compound	–R	$\log_{10}$ PGI
4	$–CH_3$	1.51
5	$–CH_2CH_2CH_2CH_3$	1.92
6	$–CH_2(CH_2)_4CH_3$	1.98
7	$–CH_2(CH_2)_5CH_3$	1.97
8	$–CH_2(CH_2)_6CH_3$	1.92

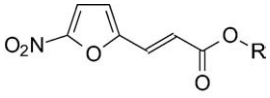

Compound	–R	$\log_{10}$ PGI
9	–H	1.30
10	$–CH_3$	1.59
11	$–CH_2CH_2CH_2CH_3$	1.62

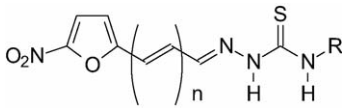

Compound	*n*	–R	$\log_{10}$ PGI
12	0	–H	1.78
13		$–CH_3$	1.69
14		$–CH_2CH_3$	1.80
15		–Ph	1.08
16	1	–H	1.87
17		$–CH_3$	1.78
18		$–CH_2CH_3$	1.86
19		–Ph	1.82

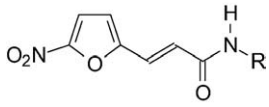

Compound	–R	$\log_{10}$ PGI
20	$–CH_2CH_2CH_2CH_3$	1.88
21	$–CH_2(CH_2)_4CH_3$	1.91
22	$–CH_2CH_2OCH_3$	1.49
23	$–CH_2$-furyl	1.15
24	$–CH_2CO_2CH_2CH_3$	1.54
25		0.78

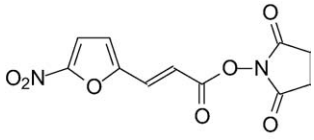

[a] PGI: percentage of growth inhibition at 5 μM.

ability to inhibit growth of the parasite, percentage of growth inhibition (PGI), was evaluated in comparison to the control (no drug added to the media) at day 5. Nfx was used as the reference trypanocidal drug (Table 2). The ID_{50} concentration (50% inhibitory dose) was assessed for compounds presenting high trypanocidal activity in each family and Nfx (Fig. 1).

4. CoMFA studies

3D-QSAR analysis was performed using the CoMFA module implemented in SYBYL 6.9 package [35,36]. The 5-nitrofuryl derivatives used in the 3D-QSAR studies were derivatives **1–40** (Tables 1 and 2). As the dependent variable in the linearisation procedure, we used $\log_{10}$ PGI values, gathered in Tables 1 and 2. In the equations and models, *n* represents the number of data points, r^2 is the correlation coefficient, q^2 represents the leave-one-out cross-validated r^2 value, SEE defines the standard error of estimate, SEP defines the standard error of prediction and the *F* value is related to the *F*-statistic analysis (Fischer test).

For systems in which no information exists about the binding site, it is a well-established assumption to consider that a similar class of molecules (congeneric series) binds to the putative receptor site adopting a similar geometry and orientation. This was done by RMS fitting of the atoms to the template molecule, derivative **1**, as it is indicated in Fig. 2a. The steric and electrostatic potential fields for CoMFA were calculated at each lattice intersection of a regularly spaced grid of 2.0 Å. The steric and electrostatic contributions were truncated as indicated in Table 3 and the electrostatic contributions were ignored at lattice intersections with maximum steric interactions. The partial-least-squares (PLS) method [37] was used to derive a linear relationship between the biological activities and the molecular fields. Leave-one-out cross validation with 2.0 kcal mol^{-1} column filtering was performed by omitting from the analysis those columns (lattice points) with an energy variance less than this threshold. This allowed determination of the optimum number of components associated with the lowest standard error of prediction.

Only models having a value of cross-validated r^2 (q^2) above 0.5 were considered (models I-VI, Table 3). It is widely accepted that a correlation with a q^2 value greater than 0.5–0.6 is useful for the prediction of new biologically active molecules [38]. The best generated models were validated using two different test set of derivatives, for model V molecules **6**, **11**, **25**, **26**, **33**, **37**, and **39** ($r = 0.785$, $s = 0.048$, $p = 0.0367$) and for model VI molecules **11**, **25**, **26**, **37**, and **39** were used ($r = 0.689$, $s = 0.059$, $p = 0.1983$). The calculated activities of the test set compounds, predicted with these models are provided in Table 4.

Models II–VI with good statistic parameters (i.e. r^2, q^2, SEP, *F* value and the number of components) are quite similar, being the electrostatic terms always a little more important than

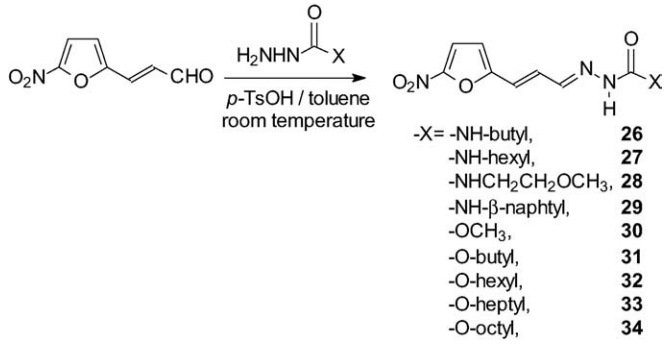

Scheme 2. Synthetic procedure for the preparation of new semicarbazone and carbazate derivatives.

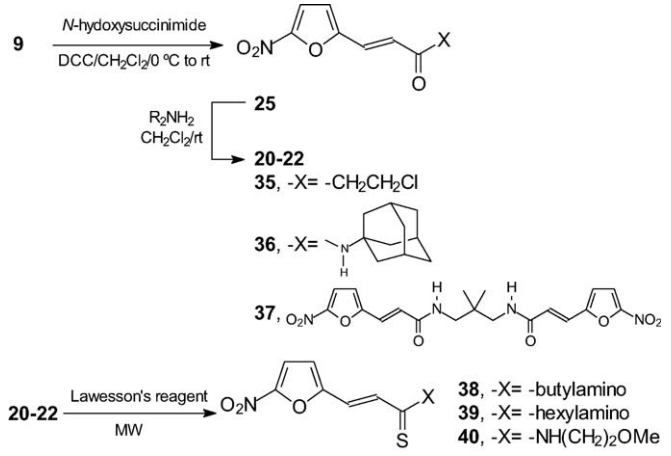

Scheme 3. Synthetic procedure for the preparation of 5-nitrofuryl derivatives **35–40**.

steric terms. The model generated using 32 molecules with lower SEE (0.050) and SEP (0.151) and higher q^2 (0.725) was selected as the best model to explain the SAR (model VI).

To visualize the CoMFA results, the CoMFA contour maps were created by using the data from PLS analysis of model VI. These maps help to explain the steric and electrostatic features of the compounds included in our analysis. The steric contour maps are shown as green and yellow polyhedra in Fig. 3a, with the green ones indicating regions in which steric bulk increase inhibitory activity. The yellow polyhedra represent regions in which steric bulk is detrimental to the activity. The green polyhedra may be envisioned as hydrophobic cavities in some receptor, which can accommodate hydrophobic groups. In contrast, the yellow polyhedra represent areas already occupied by the receptor, which would thus prohibit any effective binding. The electrostatic contour maps (Fig. 3b) illustrate with red polyhedra the areas in which electron-rich groups lead to increase of biological activities. These may be envisioned as electropositive groups within the active pocket of some biological receptor. In contrast, the blue contours represent electron-deficient regions and may be visualized as the electronegative groups in the active pocket.

5. Discussion

The new 5-nitrofuran derivatives developed show excellent anti-trypanosomal activity. The most active derivatives (semicarbazone **27**, carbazates **31–34** and amide **36**) displayed ID_{50} between 2.0 and 3.0 times lower than Nfx. The most potent compound is the heptyl carbazate **33**. In general, the carbazate derivatives were more active than the semicarbazone analogues (compare semicarbazones **1**, **26** and **27** activities with carbazates **5**, **31** and **32** activities). While, 5-nitrofurylacrolein derivatives were more active than 5-nitrofuryl ones (compare activities for 5-nitrofuryl derivatives **1**, **5** and **8** and 5-nitrofurylacrolein derivatives **26**, **31** and **34** activities).

The presence of apolar chains in each family of derivatives resulted in more active compounds than the less apolar ones (i. e. compare activities of semicarbazones **27** and **28**, and carbazates **34** and **30**). The amide **36**, displaying an apolar adamantyl moiety, is the best trypanocidal 5-nitrofurylpropenamide developed until now. On the other hand, thioamides were less active than the amides analogues (compare derivatives **38–40** activities with parent amides **20–22** activities). Derivatives **41** and **42**, substituted with a polar heterocycle, were inactive at 5 μM.

The 3D-QSAR studies performed showed that steric requirements were localized around the substituent bonded to carbonyl or thiocarbonyl moieties with sterically favourable contours approximately 5 Å around these functionalities. Accordingly, the optimum length of the molecule, from the nitro group, was near to 17 Å. Bulky groups, like naphthyl and furfuryl, located near carbonyl and thiocarbonyl moieties, 10 Å away from nitro moiety, decrease the anti-parasitic activity (yellow polyhedra, Fig. 3a).

Regarding the electrostatic field effects on activity, two main regions in the molecule could be recognized, the lateral chain and the carbonyl or thiocarbonyl moiety. The discriminating power of the electrostatic field around the heterocyclic ring was poor, because the molecules were aligned as shown in Fig. 2. The 3D-QSAR indicated that a favourable electron-deficient region (blue contour, Fig. 3b), 14–15 Å from the nitro

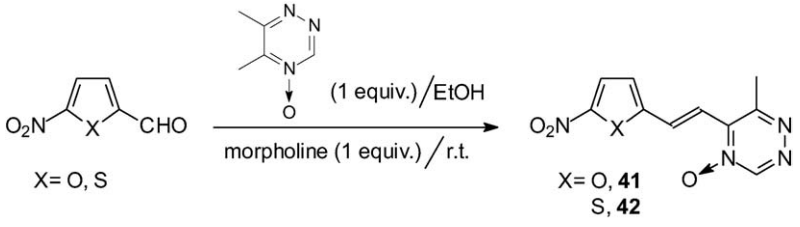

Scheme 4. Synthetic procedure for the preparation of derivatives **41–42**.

Table 2
In vitro biological activity of new 5-nitrofuryl derivatives

Compound	PGI (%) [a,b]	$\log_{10}$ PGI
26	58	1.76
27	82	1.91
28	27	1.43
29	24	1.38
30	58	1.76
31	87	1.94
32	86	1.93
33	90	1.95
34	92	1.96
35	60	1.78
36	91	1.96
37	47	1.67
38	52	1.72
39	11	1.04
40	12	1.08
41	30	1.48
42	0	–
Nfx	46	–

[a] PGI: percentage of growth inhibition at 5 μM. [b] The results are the means of three different experiments with an S.D. less than 10% in all cases.

moiety, is important for the activity. This region corresponds, in the most active derivatives, to a hydrocarbon backbone (alkyl, adamantyl, aryl). A clear electron-rich region, near to the carbonyl or thiocarbonyl group, also increases the activity. In the active site of Trypanothione reductase, a proposed target for this family of compounds [14,20], this region is involved in hydrogen bonding interactions. In consequence, amides, thioamides and esters, presenting different patterns of hydrogen bonding, have different activities. In general, amides derivatives, i.e. derivative **20** ($\log_{10}$ PGI = 1.88), were more active than the corresponding ester, i.e. derivative **11** ($\log_{10}$ PGI = 1.62), and thioamide analogues, i.e. derivative **38** ($\log_{10}$ PGI = 1.72). CoMFA results points to the importance of a specific hydrogen-bonding pattern around the carbonyl or thiocarbonyl moieties, as well as the requirement for hydrophobic lateral chains.

6. Conclusions

The results presented above indicate that the in vitro activity of new 5-nitrofuryl derivatives against Tulahuen 2 strain of *T. cruzi* is superior to that of the nitrofuran commercially used in the past (Nfx). However, to consider the potential use of these derivatives as drugs they should present adequate behaviour in vivo. To assess this the fulfilment of Lipinski rules [39] and the value of topological polar surface area (TPSA) [40,41] were analysed. Lipinski described desired ranges for certain properties thought to be important for pharmacokinetics and drug development. They are: *C* log *P* < 5, number of hydrogen bond donors ≤ 5, number of hydrogen bond acceptors ≤ 10, and molecular weight < 500. A compound that fulfils at least three out of four of these criteria adhere to Lipinski's rule.

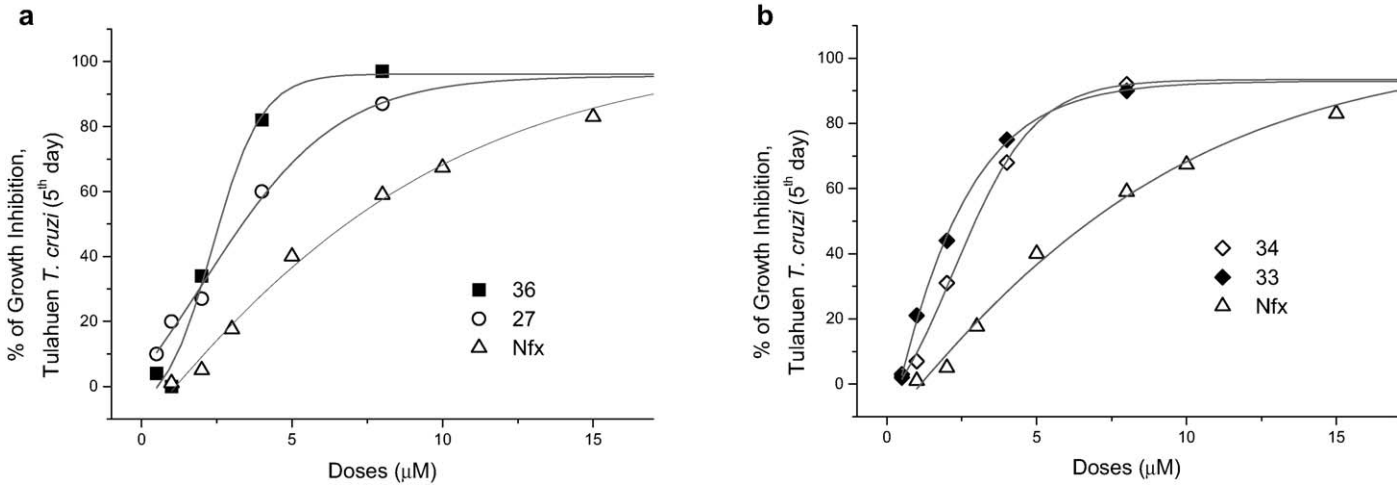

Fig. 1. Curves dose-response of Nfx and derivatives **27**, **33**, **34**, and **36**. ID_{50} (μM) (± 0.5): **27**, 3.4; **33**, 2.3; **34**, 3.0; **36**, 2.6; **Nfx**, 6.1.

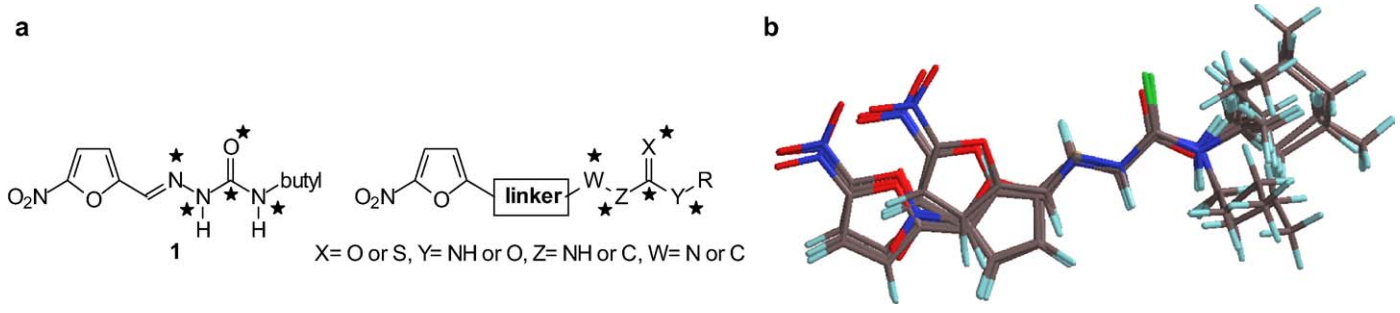

Fig. 2. **a)** Atoms used to align CoMFA molecules. **b)** Stereoview of some aligned molecules used in the CoMFA study.

Table 3
PLS results of CoMFA models

CoMFA Model	PLS analysis						Contribution		n	Compounds
	q^2	Components	SEP	r^2	SEE	F value	Steric [a]	Electrostatic [a]		
I	0.549	4	0.158	0.882	0.081	39.17	62.6 [b]	37.4 [b]	26	**2–7**, **10**, **11**, **11–19**, **21**, **26–34**
II	0.634	6	0.169	0.940	0.067	72.66	49.7 [b]	50.3 [b]	34	**2–8**, **10**, **11**, **12–21**, **23**, **24**, **26–36**, **38**, **40**
III	0.636	6	0.168	0.940	0.067	72.70	48.6 [c]	51.4 [c]	34	**2–8**, **10**, **11**, **12–21**, **23**, **24**, **26–36**, **38**, **40**
IV	0.664	6	0.164	0.950	0.061	88.44	49.8 [b]	50.2 [b]	33	**2–8**, **10**, **12–21**, **23**, **24**, **26–36**, **38**, **40**
V	0.711	6	0.160	0.970	0.050	130.06	48.0 [b]	52.0 [b]	30	**2–5**, **7**, **8**, **10**, **12–21**, **23**, **24**, **27–32**, **34–36**, **38**, **40**
VI	0.725	6	0.151	0.970	0.050	134.98	48.0 [b]	52.0 [b]	32	**2–8**, **10**, **12–21**, **23**, **24**, **27–36**, **38**, **40**

[a] Contribution truncated to: [b] ± 30 kcal mol^{-1} [c] ± 20 kcal mol^{-1}.

Table 4
Predicted anti *T. cruzi* activity using CoMFA models V and VI

Compound	$\log_{10}$GPI	CoMFA calculated [a]	CoMFA calculated [b]
6	1.98	1.92	–
11	1.62	1.84	1.83
25	0.78	1.84	1.84
26	1.76	1.97	1.97
33	1.95	1.97	–
37	1.67	1.92	1.92
39	1.04	1.79	1.80

[a] CoMFA predicted biological activity using model V.
[b] CoMFA predicted biological activity using model VI.

Another very helpful parameter for the prediction of absorption is the polar surface area (PSA), defined as the sum of surfaces of polar atoms in a molecule, which provides good correlation with experimental transport data (intestinal absorption, Caco-2 monolayers penetration, and blood-brain barrier crossing) [41]. Table 5 lists such physicochemical properties for the most promising trypanocidal 5-nitrofuryl derivatives. All of the potent antiparasitic 5-nitrofuryl derivatives presented herein are fully compatible with Lipinski's rules and posses similar or better TPSA than nifurtimox, providing supporting evidence for further in vivo studies.

7. Experimental

7.1. Chemistry

All starting materials were commercially available research-grade chemicals and used without further purification. Compounds **9**, **20–22**, **25**, and **41–42** and semicarbazide and carbazate reactants were prepared following literature procedures [14,23,24,30,31]. All solvents were dried and distilled prior to use. All the reactions were carried out in a nitrogen atmosphere. Melting points were determined using a Leitz Microscope Heating Stage Model 350 apparatus and are uncorrected. Elemental analyses were obtained from vacuum-dried samples (over phosphorous pentoxide at 3–4 mmHg, 24 h at room temperature) and performed on a Fisons EA 1108 CHNS-O analyser. Infrared spectra were recorded on a Perkin Elmer 1310 apparatus, using potassium bromide tablets; the frequencies are expressed in cm^{-1}. ^{1}H-NMR and ^{13}C-NMR spectra were recorded on a Bruker DPX-400 (at 400 and 100 MHz) instrument, with tetramethylsilane as the internal reference and in the indicated solvent; the chemical shifts are reported in ppm. J values are given in Hz. Mass spectra were recorded on a Shimadzu GC-MS QP 1100 EX instrument at 70 eV.

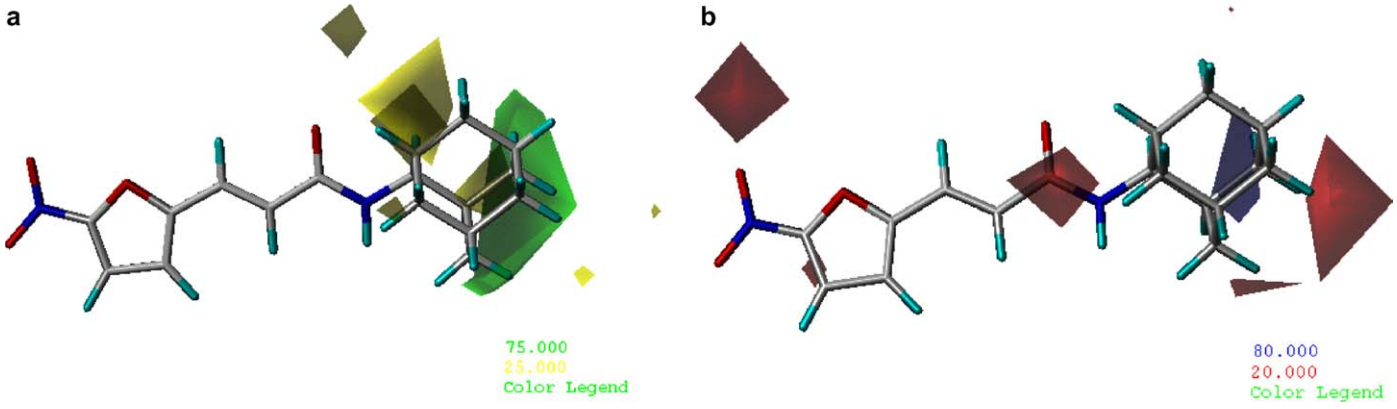

Fig. 3. **a)** Views of the CoMFA steric field contour maps for the model VI, the steric field was contoured at 0.075 and –0.075 levels. Compound **36** is superimposed in the map. **b)** Views of the CoMFA electrostatic field contour maps for the model VI, the electrostatic field was contoured at 0.075 and –0.075 levels. Compounds **36** is superimposed in the maps.

Table 5
Nfx and 5-nitrofuryl derivatives' properties described to fulfil Lipinski rule

Reference	Lipinski rule					TPSA [b,c]
	C log P [a]	Number of H-bond donors [b]	Number of H-bond acceptors [b]	Molecular weight	Number of criteria met	
Rule	< 5	≤ 5	≤ 10	< 500	at least 3	
21	4.81	1	6	266.3	all	88.1
27	2.82	2	8	308.3	all	112.5
32	4.31	1	8	309.3	all	109.7
33	4.65	1	8	323.3	all	109.7
36	4.57	1	6	316.1	all	88.1
39	5.77	1	5	282.1	3	71.0
Nfx	8.51	0	8	287.0	3	108.7

[a] Theoretical logP (*C* log *P*) was calculated using Villar method, at AM1 semiempirical method, implemented in Spartan'04, 1.0.1 version, suite of programs [42].
[b] http://www.molinspiration.com/cgi-bin/properties.
[c] TPSA: topological polar surface area.

*7.1.1. General procedure for the synthesis of **26–34***

A mixture of 3-(5-nitrofuryl)acroleine) (1 equiv.), the corresponding semicarbazide or carbazate reactant (1 equiv.), *p*-TsOH (catalytic amounts) and toluene as solvent was stirred at room temperature until the carbonyl compound was not present (SiO_2, 1% MeOH in CH_2Cl_2). The resulting precipitate was collected by filtration and was crystallized from the indicated solvent.

*7.1.1.1. 4-(Butyl)-1-[3-(5-nitrofuryl)-2E-propen-1E-ilidene] semicarbazide (**26**)*. Orange-brown solid (62%); m.p. 163.3–165.0 °C (from toluene) (Found: C, 51.8; H, 6.0; N, 19.7. $C_{12}H_{16}N_4O_4$ requires C, 51.4; H, 5.8; N, 20.0); δ_H (400 MHz , $CDCl_3$) 0.97 (3 H, t, *J* 7.4, –CH_2CH_3), 1.41 (2 H, sextet, *J* 7.2, –$CH_2CH_2CH_3$), 1.58 (2 H, quintet, *J* 7.4, –$NCH_2CH_2CH_2$), 3.34 (2 H, q, *J* 7.0, -NCH_2), 6.11 (1H, br t, –$NHCH_2$), 6.55 (1 H, d, *J* 4.0, furan-*H*), 6.57 (1H, d, *J* 16.2, –C*H*=), 7.09 (1H, dd, J_1 9.5, J_2 16.0, –C*H*=), 7.33 (1 H, d, *J* 3.8, furan-*H*), 7.54 (1 H, d, *J* 9.5, –C*H*=N) and 9.79 (1 H, br s, N*H*); δ_C (100 MHz, $CDCl_3$) (HMQC, HMBC) 14.16, 20.42, 32.56, 39.95 (butyl group), 112.21 (furan-*C*), 114.11 (furan-*C*), 121.34 (–*C*H=), 130.94 (–*C*H=),140.66 (H–*C*=N), 152.18 (furan-*C*), 155.01 (furan-*C*) and 156.52 (–*C*=O). *m/z* 280 ($M^{\cdot+}$, 36.0%), 207 (5.0) and 181 (100.0).

*7.1.1.2. 4-(Hexyl)-1-[3-(5-nitrofuryl)-2E-propen-1E-ilidene] semicarbazide (**27**)*. Yellow-orange needles (58%); m.p. 174.3–175.8 °C (from toluene) (Found: C, 54.9; H, 6.7; N, 17.9. $C_{14}H_{20}N_4O_4$ requires C, 54.5; H, 6.5; N, 18.2); δ_H (400 MHz, CD_3OD) 0.92 (3 H, m, –CH_2CH_3), 1.36 (6 H, m, –$CH_2CH_2CH_2CH_3$), 1.57 (2 H, m, –$NCH_2CH_2CH_2$), 3.26 (2 H, t, *J* 7.1, –NCH_2), 6.70-6.90 (3H, m, –$NHCH_2$ + furan-*H* + –C*H*=), 7.11 (1H, dd, J_1 9.4, J_2 16.0, –C*H*=), 7.49 (1 H, d, *J* 3.8, furan-*H*), 7.66 (1 H, d, *J* 9.4, –C*H*=N) and 9.78 (1 H, br s, -N*H*); δ_C (100 MHz, CD_3OD) (HMQC, HMBC) 13.33, 22.64, 26.61, 30.22, 31.72, 39.74 (hexyl group), 112.46 (furan-*C*), 113.90 (furan-*C*), 121.66 (–*C*H=), 130.53 (–*C*H=),141.55 (H–*C*=N), 152.00 (furan-*C*), 155.00 (furan-*C*) and 155.27 (–*C*=O). *m/z* 308 ($M^{\cdot+}$, 25.0%), 207 (2.0) and 181 (60.0).

*7.1.1.3. 4-(2-Methoxyethyl)-1-[3-(5-nitrofuryl)-2E-propen-1E-ilidene]semicarbazide (**28**)*. Orange needles (80%); m.p. 171.5–173.0 °C (from toluene) (Found: C, 47.0; H, 5.3; N, 19.6. $C_{11}H_{14}N_4O_5$ requires C, 46.8; H, 5.0; N, 19.9); δ_H (400 MHz, $CDCl_3$) 3.43 (3 H, s, –OCH_3), 3.55 (4 H, m, –$NCH_2CH_2OCH_3$), 6.43 (1H, br t, –$NHCH_2$), 6.58 (1 H, d, *J* 4.0, furan-*H*), 6.60 (1H, d, *J* 15.0, –C*H*=), 7.12 (1H, dd, J_1 9.5, J_2 16.1, –C*H*=), 7.35 (1 H, d, *J* 3.8, furan-*H*), 7.55 (1 H, d, *J* 9.5, –C*H*=N) and 9.65 (1 H, s, –N*H*). *m/z* 282 ($M^{\cdot+}$, 33.0%), 207 (6.0) and 181 (73.0).

*7.1.1.4. 4-(2-Naphthyl)-1-[3-(5-nitrofuryl)-2E-propen-1E-ilidene]semicarbazide (**29**)*. Brilliant brown-orange needles (80%); m.p. > 230.0 °C (from ethanol) (Found: C, 62.0; H, 4.2; N, 15.7. $C_{18}H_{14}N_4O_4$ requires C, 61.7; H, 4.0; N, 16.0); δ_H (400 MHz, DMSO-d_6) 6.57 (1 H, d, *J* 3.9, furan-*H*), 6.59 (1H, d, *J* 15.9, –C*H*=), 7.15 (1H, dd, J_1 9.6, J_2 16.0, –C*H*=), 7.35 (1 H, d, *J* 4.0, furan-*H*), 7.41 (1 H, dt, J_1 1.0, J_2 7.9, naphthyl-*H*), 7.50-7.75 (3 H, m, –C*H*=N + naphthyl-*H* + naphthyl-*H*), 7.83 (2 H, m, naphthyl-*H* + naphthyl-*H*), 7.85 (1 H, d, *J* 9.1, naphthyl-*H*), 8.19 (1 H, d, *J* 1.9, naphthyl-*H*), 9.00 (1 H, s, N*H*) and 11.00 (1 H, s, N*H*). *m/z* 350 ($M^{\cdot+}$, 35.0%), 207 (11.0), 181 (21.0) and 143 (100.0).

*7.1.1.5. Methyl 4-[3-(5-nitrofuryl)-2E-propen-1E-ilidene]carbazate (**30**)*. Orange-brown solid (50%); m.p. 224.2–226.8 °C (from toluene) (Found: C, 45.1; H, 3.6; N, 17.4. $C_9H_9N_3O_5$ requires C, 45.2; H, 3.8; N, 17.6); δ_H (400 MHz , DMSO-d_6) 3.76 (3 H, s, O-CH_3), 6.59 (1 H, d, *J* 3.8, furan-*H*), 6.61 (1H, d, *J* 16.0, –C*H*=), 7.17 (1H, dd, J_1 9.5, J_2 15.9, –C*H*=), 7.33 (1 H, d, *J* 3.7, furan-*H*), 7.65 (1 H, br s, –C*H*=N) and 8.20 (1 H, br s, N*H*). *m/z* 239 ($M^{\cdot+}$, 87.0%), 207 (2.1), and 181 (0.2).

*7.1.1.6. Butyl 4-[3-(5-nitrofuryl)-2E-propen-1E-ilidene]carbazate (**31**)*. Yellow-orange solid (52%); m.p. 138.0–140.0 °C

(from toluene) (Found: C, 51.1; H, 5.2; N, 14.8. $C_{12}H_{15}N_3O_5$ requires C, 51.2; H, 5.4; N, 14.9); δ_H (400 MHz , $CDCl_3$) 0.95 (3 H, t, *J* 7.2, –CH_2CH_3), 1.41 (2 H, sextet, *J* 7.3, –$CH_2CH_2CH_3$), 1.69 (2 H, m, –$OCH_2CH_2CH_2$), 4.26 (2 H, t, *J* 6.0, –OCH_2), 6.60 (1 H, d, *J* 3.6, furan-*H*), 6.62 (1H, d, *J* 15.7, –C*H*=), 7.18 (1H, dd, J_1 9.4, J_2 16.1, –C*H*=), 7.32 (1 H, d, *J* 3.5, furan-*H*), 7.68 (1 H, br s, –C*H*=N) and 8.50 (1 H, br s, N*H*). *m/z* 281 ($M^{\cdot+}$, 44.0%), 207 (7.5), and 181 (12.6).

*7.1.1.7. Hexyl 4-[3-(5-nitrofuryl)-2E-propen-1E-ilidene]carbazate (**32**)*. Yellow solid (37%); m.p. 154.6–156.4 °C (from toluene) (Found: C, 54.3; H, 6.2; N, 13.7. $C_{14}H_{19}N_3O_5$ requires C, 54.4; H, 6.2; N, 13.6); δ_H (400 MHz , $CDCl_3$) (COSY) 0.90 (3 H, t, *J* 6.8, –CH_2CH_3), 1.33 (6 H, m, –$CH_2CH_2CH_2CH_3$), 1.70 (2 H, quintet, *J* 6.9, –$OCH_2CH_2CH_2$), 4.24 (2 H, t, *J* 6.7, –OCH_2), 6.60 (1 H, d, *J* 3.8, furan-*H*), 6.61 (1H, d, *J* 16.0, –C*H*=), 7.19 (1H, dd, J_1 9.3, J_2 16.0, –C*H*=), 7.32 (1 H, d, *J* 3.8, furan-*H*), 7.70 (1 H, br s, –C*H*=N) and 8.40 (1 H, br s, N*H*); δ_C (100 MHz, $CDCl_3$) (HMQC, HMBC) 14.35, 22.90, 25.76, 29.20, 31.79, 67.00 (hexyl group), 112.21 (furan-*C*), 113.93 (furan-*C*), 122.90 (–*C*H=), 130.64 (–*C*H=),144.00 (H–*C*=N), 152.00 (furan-*C*), 154.00 (furan-*C*) and 154.74 (–*C*=O). *m/z* 281 ($M^{\cdot+}$, 44.0%), 207 (7.5), and 181 (12.6).

*7.1.1.8. Heptyl 4-[3-(5-nitrofuryl)-2E-propen-1E-ilidene]carbazate (**33**)*. Yellow solid (50%); m.p. 151.9–152.6 °C (from petroleum ether/ethyl acetate) (Found: C, 55.7; H, 6.4; N, 12.9. $C_{15}H_{21}N_3O_5$ requires C, 55.7; H, 6.6; N, 13.0); ν_{max} 3215.7, 1716.9, 1558.7, 1348.4 and 810.2; δ_H (400 MHz , $CDCl_3$) 0.89 (3 H, t, *J* 7.1, –CH_2CH_3), 1.30 (8 H, m, –C$H_2CH_2CH_2CH_2CH_3$), 1.69 (2 H, m, –$OCH_2CH_2CH_2$), 4.24 (2 H, t, *J* 6.8, –OCH_2), 6.60 (1 H, d, *J* 3.8, furan-*H*), 6.61 (1H, d, *J* 16.0, –C*H*=), 7.19 (1H, dd, J_1 9.3, J_2 16.1, –C*H*=), 7.32 (1 H, d, *J* 3.8, furan-*H*), 7.62 (1 H, br s, –C*H*=N) and 8.12 (1 H, s, N*H*). *m/z* 323 ($M^{\cdot+}$, 10.0%), 207 (4.5), and 181 (1.2).

*7.1.1.9. Octyl 4-[3-(5-nitrofuryl)-2E-propen-1E-ilidene]carbazate (**34**)*. Yellow powder (15%); m.p. 146.8–148.0 °C (from petroleum ether/ethyl acetate) (Found: C, 56.9; H, 6.7; N, 12.7. $C_{16}H_{23}N_3O_5$ requires C, 57.0; H, 6.9; N, 12.5); ν_{max} 3233.1, 1709.1, 1564.5, 1350.3 and 814.1; δ_H (400 MHz , $CDCl_3$) 0.88 (3 H, t, *J* 7.1, –CH_2CH_3), 1.28 (10 H, m, –C$H_2CH_2CH_2CH_2CH_2CH_3$), 1.69 (2 H, m, –$OCH_2CH_2CH_2$), 4.24 (2 H, t, *J* 6.68, –OCH_2), 6.60 (1 H, d, *J* 3.8, furan-*H*), 6.61 (1H, d, *J* 16.0, –C*H*=), 7.19 (1H, dd, J_1 9.3, J_2 16.1, –C*H*=), 7.32 (1 H, d, *J* 3.8, furan-*H*), 7.65 (1 H, br s, –C*H*=N) and 8.15 (1 H, s, N*H*). *m/z* 337 ($M^{\cdot+}$, 10.5%), 207 (5.6), and 181 (1.7).

*7.1.2. General procedure for the synthesis of amides **35**–**37***

A mixture of intermediate **25** (1 eq.), the corresponding amine (1.2 eq.) and dry CH_2Cl_2 as solvent was stirred at room temperature until the compound **25** was not present (SiO_2, 40% EtOAc in petroleum ether). The mixture was concentrated in vacuo and treated with EtOAc. After the work-up process the residue was purified as indicate.

*7.1.2.1. N-(2-chloroethyl) 3-(5-nitrofuryl)-2E-propenamide (**35**)*. Chromatographic column (SiO_2, methylene chloride); beige solid (53%); m.p. 143.0–145.0 °C; (Found: C, 43.9; H, 3.4; N, 14.2. $C_9H_9ClN_2O_4$ requires C, 44.2; H, 3.7; N, 14.5); δ_H (400 MHz, acetone-d_6) 3.66 (2 H, m, –CH_2), 3.74 (2 H, m, –CH_2), 6.87 (1 H, d, *J* 15.6, =C*H*–), 7.07 (1 H, d, *J* 3.8, furan-*H*), 7.43 (1 H, d, *J* 15.6, =C*H*–), 7.58 (1 H, d, *J* 3.8, furan-*H*) and 7.88 (1 H, br s, N*H*); *m/z* 244/246 ($M^{\cdot+}$, 28.0/10.0%), 227/229 (13.0/4.3) and 166 (100.0).

*7.1.2.2. N-(1-adamantyl) 3-(5-nitrofuryl)-2E-propenamide (**36**)*. Chromatographic column (SiO_2, petroleum ether); beige solid (40%); m.p. 145.0 °C (dec.); (Found: C, 64.8; H, 6.7; N, 8.6. $C_{17}H_{20}N_2O_4$ requires C, 64.5; H, 6.4; N, 8.9); δ_H (400 MHz, $CDCl_3$) 1.74 (6 H, m, –CH_2), 2.08 (6 H, m, –CH_2), 2.14 (3 H, m, –C*H*), 5.43 (1 H, br s, N*H*), 6.61 (1 H, d, *J* 15.3, =C*H*–), 6.67 (1 H, d, *J* 3.8, furan-*H*), 7.33 (1 H, d, *J* 15.2, =C*H*–) and 7.34 (1 H, d, *J* 3.8, furan-*H*); δ_C (100 MHz, $CDCl_3$) (HMQC, HMBC) 29.82, 36.69, 41.99, 53.07 (adamantyl group), 113.57 (furan-*C*), 114.82 (furan-*C*), 125.30 (–*C*H=), 127.24 (–*C*H=), 151.00 (furan-*C*), 153.76 (furan-*C*) and 163.36 (–*C*=O); *m/z* 316 ($M^{\cdot+}$, 4.0%), 301 (8.0) and 166 (88.0).

*7.1.2.3. 2,2-Dimethyl-N,N′-bis[3-(5-nitrofuryl)-2E-propenoyl] propan-1,3-diamine (**37**)*. Chromatographic column (SiO_2, petroleum ether/ethyl acetate (0–40%)); yellow oil (37%); (Found: C, 52.4; H, 4.4; N, 12.8. $C_{19}H_{20}N_4O_8$ requires C, 52.8; H, 4.7; N, 13.0); δ_H (400 MHz, $CDCl_3$) 0.99 (6 H, s, –CH_3), 3.20 (4 H, d, *J* 6.9, N–CH_2), 6.74 (1 H, d, *J* 3.5, furan-*H*), 6.76 (1 H, d, *J* 15.0, =C*H*–), 6.96 (1 H, br t, *J* 6.8, N*H*), 7.37 (1 H, d, *J* 3.8, furan-*H*) and 7.47 (1 H, d, *J* 15.3, =C*H*–); *m/z* 432 ($M^{\cdot+}$, 5.5%), 417 (3.9) and 166 (44.0).

*7.1.3. General procedure for the synthesis of thioamides **38**–**40***

A mixture of the corresponding amides (**20**–**22**) (1 eq.) and Lawesson's reagent (1 eq.) was microwave irradiated for 2 min three times. The mixture was purified as indicate.

*7.1.3.1. N-butyl 3-(5-nitrofuryl)-2E-propenthioamide (**38**)*. Chromatographic column (SiO_2, petroleum ether); yellow oil (27%); (Found: C, 51.6; H, 5.3; N, 10.8; S, 12.2. $C_{11}H_{14}N_2O_3S$ requires C, 52.0; H, 5.6; N, 11.0; S, 12.6); δ_H (400 MHz, $CDCl_3$) 1.01 (3 H, t, *J* 7.4, –CH_3), 1.47 (2 H, sextet, *J* 7.3, –CH_2), 1.74 (2 H, quintet, *J* 7.7, –CH_2), 3.82 (2 H, t, *J* 7.3, N-CH_2), 6.75 (1 H, d, *J* 3.8, furan-*H*), 6.99 (1 H, d, *J* 15.0, =C*H*–), 7.35 (1 H, d, *J* 3.8, furan-*H*), 7.44 (1 H, br s, N*H*) and 7.69 (1 H, d, *J* 15.0, =C*H*–); *m/z* 254 ($M^{\cdot+}$, 0.5%), 225 (1.4) and 182 (1.9).

*7.1.3.2. N-hexyl 3-(5-nitrofuryl)-2E-propenthioamide (**39**)*. Chromatographic column (SiO_2, petroleum ether); brown-yellow oil (15%); (Found: C, 55.0; H, 6.1; N, 9.6; S, 11.0.

$C_{13}H_{18}N_2O_3S$ requires C, 55.3; H, 6.4; N, 9.9; S, 11.4); δ_H (400 MHz, $CDCl_3$) 0.91 (3 H, t, *J* 7.0, -C*H*$_3$), 1.33 (4 H, m, -C*H*$_2$C*H*$_2$CH$_3$), 1.40 (2 H, m, –C*H*$_2$CH$_2$), 1.72 (2 H, quintet, *J* 7.6, –C*H*$_2$CH$_2$), 3.79 (2 H, q, *J* 7.2, N–C*H*$_2$), 6.72 (1 H, d, *J* 3.8, furan-*H*), 6.97 (1 H, d, *J* 15.0, =C*H*–), 7.33 (1 H, d, *J* 3.8, furan-*H*), 7.38 (1 H, br s, N*H*) and 7.67 (1 H, d *J* 15.0, =C*H*–). *m/z* 282 ($M^{\cdot+}$, 12.0%), 265 (7.4) and 182 (17.7).

*7.1.3.3. N-(2-methoxyethyl) 3-(5-nitrofuryl)-2E-propenthioamide (**40**)*. Chromatographic column (SiO_2, petroleum ether/ethyl acetate (0–10%)); yellow oil (12%); (Found: C, 46.6; H, 4.8; N, 11.0; S, 12.4. $C_{10}H_{12}N_2O_4S$ requires C, 46.9; H, 4.7; N, 10.9; S, 12.5); δ_H (400 MHz, $CDCl_3$) 3.41 (3 H, s, O–C*H*$_3$), 3.54 (2 H, m, –C*H*$_2$OCH$_3$), 3.80 (2 H, m, N–C*H*$_2$), 6.73 (1 H, d, *J* 3.8, furan-*H*), 6.98 (1 H, d, *J* 15.1, =C*H*–), 7.34 (1 H, d, *J* 3.8, furan-*H*), 7.40 (1 H, br s, N*H*) and 7.68 (1 H, d *J* 15.1, =C*H*–). *m/z* 256 ($M^{\cdot+}$, 2.1%), 224 (5.9) and 182 (23.0).

7.2. Biology

The Tulahuen 2 strain stocks of *T. cruzi* were used in this study. Handling of live *T. cruzi* was done according to established guidelines [43]. The epimastigote form of the parasite was grown at 28 °C in an axenic medium (BHI-Tryptose), complemented with 10% foetal calf serum. Cells from a 5-day-old culture were inoculated into 50 ml of fresh culture medium to give an initial concentration of 1×10^6 cells per ml. Cell growth was followed by daily measuring the absorbance of the culture at 600 nm for 11 days. Before inoculation, the media was supplemented with 5 μM solutions of compounds from a stock DMSO solution. The final DMSO concentration in the culture media never exceeded 0.4% (vol/vol) and had no effect by itself on the proliferation of the parasites (no effect on epimastigote growth was observed by the presence of up to 1% DMSO in the culture media). The compounds ability to inhibit growth of the parasite was evaluated, in triplicate, in comparison to the control (no drug added to the media). The control was run in the presence of 0.4% DMSO and in the absence of any drug. The percentage of inhibition was calculated as follows: $\% = \{1 - [(A_p - A_{0p})/(A_c - A_{0c})]\} \times 100$, where $A_p = A_{600}$ of the culture containing the drug at day 5; $A_{0p} = A_{600}$ of the culture containing the drug just after addition of the inocula (day 0); $A_c = A_{600}$ of the culture in the absence of any drug (control) at day 5; $A_{0c} = A_{600}$ in the absence of the drug at day 0. The 50% effective concentrations (ID_{50}) were obtained. Nifurtimox (Lampit^R, Bay 2502, obtained from Bayer) was used as the reference trypanocidal drug.

7.3. 3D-QSAR

Structural manipulations were performed using SYBYL 6.9 with standard Tripos force field [35]. Molecules were built using standard parameters from the SYBYL package. All CH=CH and CH=N– bonds were considered as *E*-forms. Minimum energy geometries were obtained using Powell method until a root-mean-square (RMS) deviation of 0.001 kcal mol^{-1} Å was achieved. Partial atomic charges required for calculation of the electrostatic interaction were computed by the semi-empirical molecular orbital method using the MOPAC package [44,45]. The charges were computed using the MNDO method. The net charge of derivatives was assigned as 0 e.u.

Acknowledgements

This work received financial support from Fondo Clemente Estable (Uruguay), CSIC/UdelaR (Uruguay) and CNPq/PROSUL (Brazil). M.B. thanks to CNPq for a training-fellowship.

References

[1] http://www.who.int/ctd/chagas.
[2] A. Moncayo, WHO Special Program for Research and Training in Tropical Diseases (TDR); World Health Organization Ed, in: Eleventh Programme Report of the UNPD, World Bank, Geneva, 1993, pp. 67–75.
[3] W. De Souza, Curr. Pharm. Des. 4 (2002) 269–285.
[4] M. Almeida-de-Faria, E. Freymuller, W. Colli, M. Alves, J. Exp. Parasitol. 92 (1999) 263–274.
[5] J.F. Faucher, T. Baltz, K.G. Petry, Parasitol. Res. 81 (1995) 441–443.
[6] K.M. Tyler, D.M. Engman, Int. J. Parasitol. 31 (2001) 472–481.
[7] J.A. Urbina, Curr. Pharm. Des. 8 (2002) 287–295.
[8] H. Cerecetto, M. González, Curr. Top. Med. Chem. 2 (2002) 1185–1211.
[9] R. Docampo, S.N.J. Moreno, in: W.A. Pryor (Ed.), Free Radicals in Biology, Academic Press, New York, 1984, pp. 243–288.
[10] C. Viodé, N. Bettache, C. Narimantas, R.L. Krauth-Siegel, G. Chauvière, N. Bakalara, J. Périé, Biochem. Pharmacol. 57 (1999) 549–557.
[11] G. Chauviere, B. Bouteille, B. Enanga, C. de Albuquerque, S.L. Croft, M. Dumas, J. Perie, J. Med. Chem. 46 (2003) 427–440.
[12] H. Cerecetto, R. Di Maio, G. Ibarruri, G. Seoane, A. Denicola, G. Peluffo, C. Quijano, M. Paulino, Farmaco 53 (1998) 89–94.
[13] H. Cerecetto, R. Di Maio, M. González, M. Risso, G. Sagrera, G. Seoane, A. Denicola, G. Peluffo, C. Quijano, M.A. Basombrío, A.O.M. Stoppani, M. Paulino, C. Olea-Azar, Eur. J. Med. Chem. 35 (2000) 343–350.
[14] H. Cerecetto, R. Di Maio, M. González, G. Seoane, A. Duffaut, A. Denicola, M.J. Gil, V. Martínez-Merino, Eur. J. Med. Chem. 39 (2004) 421–431.
[15] G. Aguirre, L. Boiani, H. Cerecetto, M. Fernández, M. González, A. Denicola, L. Otero, D. Gambino, C. Rigol, C. Olea-Azar, M. Faúndez, Bioorg. Med. Chem. 12 (2004) 4885–4893.
[16] C. Olea-Azar, A.M. Atria, R. Di Maio, G. Seoane, H. Cerecetto, Spectrosc. Let. 31 (1998) 849–857.
[17] C. Olea-Azar, A.M. Atria, F. Mendizabal, R. Di Maio, G. Seoane, H. Cerecetto, Spectrosc. Let. 31 (1998) 99–109.
[18] C. Olea-Azar, C. Rigol, F. Mendizabal, A. Morello, J.D. Maya, C. Moncada, E. Cabrera, R. Di Maio, M. González, H. Cerecetto, Free Rad. Res. 37 (2003) 993–1001.
[19] C. Olea-Azar, C. Rigol, L. Opazo, A. Morello, J.D. Maya, Y. Repetto, G. Aguirre, H. Cerecetto, R. Di Maio, M. González, W. Porcal, J. Chil. Chem. Soc. 48 (2003) 77–79.
[20] V. Martínez-Merino, H. Cerecetto, Bioorg. Med. Chem. 9 (2001) 1025–1030.
[21] M. Paulino, F. Iribarne, M. Hansz, M. Vega, G. Seoane, H. Cerecetto, R. Di Maio, I. Caracelli, J. Zukerman-Schpector, C. Olea, A.O.M. Stoppani, M. Berriman, A.H. Fairlamb, O. Tapia, J. Mol. Struct. THEOCHEM 584 (2002) 95–105.

[22] A. Schmidt, R.L. Krauth-Siegel, Curr. Top. Med. Chem. 2 (2002) 1239–1259 (and references therein).
[23] L.A. Carpino, B.A. Carpino, A.G. Chester, R.W. Murray, A.A. Santilli, P.H. Terry, Org. Synth. Collect 5 (1973) 168–170 (John Wiley & Sons).
[24] H. Cerecetto, M. González, M. Risso, G. Seoane, A. López de Ceráin, O. Ezpeleta, A. Monge, L. Suescun, A. Mombrú, A.M. Bruno, Arch. Pharm. (Weinheim) 333 (2000) 387–393.
[25] S. Rajagoplan, P. Raman, Org. Synth. Collect 3 (1955) 425–427 (John Wiley & Sons).
[26] M.O. Abdel-Rahman, M.N. Aboul-Enein, W.M. Tadros, J. Chem, U.A.R. 12 (1969) 69–75.
[27] M. Bodanzky, A. Bodanzky, The Practice of Peptide Synthesis, 2nd ed, Longman Group Limited, London, 1978.
[28] R.S. Varma, D. Kumar, Org. Lett. 1 (1999) 697–703.
[29] G. Aguirre, H. Cerecetto, R. Di Maio, M. González, G. Seoane, A. Denicola, M.A. Ortega, I. Aldana, A. Monge, Arch. Pharm. (Weinheim) 335 (2002) 15–21.
[30] H. Cerecetto, M. González, S. Onetto, P. Saenz, O. Ezpeleta, A. López de Ceráin, A. Monge-Vega, Arch. Pharm. (Weinheim) 337 (2004) 247–258.
[31] H. Cerecetto, M. González, M. Risso, P. Saenz, C. Olea-Azar, A.M. Bruno, A. Azqueta, A. López de Ceráin, A. Monge, Arch. Pharm. (Weinheim) 337 (2004) 271–280.
[32] F. Delmas, M. Gasquet, P. Timon-David, N. Madadi, P. Vaille, J. Maldonado, Eur. J. Med. Chem. 28 (1993) 23–27.
[33] M. Hesse, H. Meier, B. Zeeh, Spektroskopishce Methoden in der organischen Chemie, 5th ed, Georg Thieme Verlag Stuttgart, New York, 1995.
[34] A. Denicola, H. Rubbo, D. Rodríguez, R. Radi, Arch. Biochem. Biophys. 304 (1993) 279–286.
[35] SYBYL, Tripos Associates, 1699 South Hanley Road, Suite 303, St. Louis, Missouri 63144.
[36] R.D. Cramer, D.E. Patterson, J. Bunce, J. Am. Chem. Soc. 110 (1988) 5959–5967.
[37] M. Clark, R.D. Cramer, Quant. Struct.-, Act. Relationships 12 (1993) 137–145.
[38] M. Boehm, J. Stuerzebecher, G. Klebe, J. Med. Chem. 42 (1999) 458–477.
[39] C.A. Lipinski, F. Lombardo, B.W. Dominy, P.J. Feeney, Adv. Drug Deliv. Rev. 23 (1997) 3–25.
[40] D.E. Clark, J. Pharm. Sci. 88 (1999) 807–814.
[41] J. Kelder, P.D.J. Grootenhuis, D.M. Bayada, L.P.C. Delbressine, J.-P. Ploemen, Pharm. Res. 16 (1999) 1514–1519.
[42] Spartan'04; Wavefunction, Inc. 18401 Von Karman Avenue, Suite 370. Irvine, California 92612 USA.
[43] L. Hudson, F. Grover, W.E. Gutteridge, R.A. Klein, W. Peters, R.A. Neal, M.A. Miles, M.T. Scott, R. Nourish, B.P. Ager, Trans. R. Soc. Trop. Med. Hyg. 77 (1983) 416–419.
[44] W.J. Hehre, L. Radom, P.V.R. Schleyer, J.A. Pople, *Ab initio* molecular orbital theory, Wiley, New York, 1986.
[45] W.J. Hehre, A.J. Shusterman, W.W. Huang, A laboratory book of computational organic chemistry, Wavefunction Inc., California, 1996.